Powder Technology 407 (2022) 117614

Contents lists available at ScienceDirect

Powder Technology

journal homepage: www.journals.elsevier.com/powder-technology

A new approach to quantify powder's bed surface roughness in additive manufacturing

Hamid Salehi [a,b,*], John Cummins [a], Enrico Gallino [c], Neil Harrison [d], Ali Hassanpour [e], Mike Bradley [a]

[a] Wolfson Centre for Bulk Solids Handling Technology, Faculty of Engineering & Science, University of Greenwich, ME4 4TB, United Kingdom
[b] School of Engineering, University of Greenwich, ME4 4TB, United Kingdom
[c] RICOH UK Products Ltd, Priorslee, Telford, United Kingdom
[d] Carpenter Additive, Widnes, United Kingdom
[e] School of Chemical and Process Engineering, University of Leeds, LS2 9JT, United Kingdom

HIGHLIGHTS

- New technique and prototype instrument developed to simulate the creation of a powder bed in Additive Manufacturing.
- Shadowgraphy technique, surface illumination with low-angle collimated light, used to quantify powder bed surface roughness.
- Two surface roughness metrics, amplitude of variation in grey-scale and wavelength of grey-scale, was developed.
- Impact of spreader shapes and gap sizes on surface roughness of six powders was studied.
- The developed tester and the techniques were successfully used to quantify powder bed surface roughness.

GRAPHICAL ABSTRACT

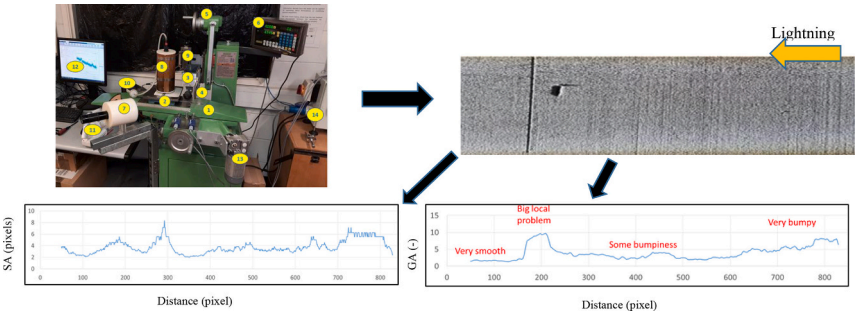

ARTICLE INFO

Keywords:
Surface roughness
Powder spreading
Flow properties
AM machine

ABSTRACT

The powder bed surface roughness plays an important role in the quality of the final parts fabricated using powder bed Additive Manufacturing processes. This paper reports the development and application of a new technique and prototype instrument which can be used to simulate the creation of a powder bed and reveal the surface properties of that bed. The tester was successfully used to study powder bed surface roughness, but can also be used to evaluate powder bed relative packing fraction, change in particle size and shape over the build plate and electrostatic charges over the powder bed. The focus of this paper is on the developments of metrics to define powder bed surface roughness. In this investigation, six plastic and two metal powders, as well as two recoater blade shape, were used. Two gap sizes of the recoaters were tested, namely two and five times higher than the powder D_{90}. A novel shadowgraphy technique based on illuminating the surface with low-angle collimated light and analysing the image was employed to quantify powder bed surface roughness. Two main

* Corresponding author at: Wolfson Centre for Bulk Solids Handling Technology, Faculty of Engineering & Science, University of Greenwich, ME4 4TB, United Kingdom.
E-mail address: hs2602e@gre.ac.uk (H. Salehi).

https://doi.org/10.1016/j.powtec.2022.117614
Received 12 January 2022; Received in revised form 25 May 2022; Accepted 7 June 2022
Available online 11 June 2022

metrics to quantify the surface roughness of the powder bed were found to be useful. The first metric is amplitude of variation in surface height which is defined as the difference between surface height at each data point and the average height over 100 points. The second metric is wavelength of roughness which is calculated as the average horizontal distance between positive peaks, averaged over 100 data points. The surface roughness results showed that the shadowgraphy technique as well as the metrics developed by this method to quantify powder bed surface roughness, are capable of quantifying and distinguishing various powder bed features (and therefore potential quality failures in the bed). These metrics successfully captured the impact of different spreading variables; i.e. recoater shape, gap size and particularly the powder flow functions on the powder bed surface roughness.

1. Introduction

Additive manufacturing (AM) represents a rapidly growing set of manufacturing processes with extensive research activities dedicated to further developing its potential. In Additive Layer Manufacturing (ALM), often a controlled laser or electron beam is used for the sintering/melting of powders spread over the build plate; alternatively a binder may be jetted into the layer to bond the particles together, or an infra-red image projected onto the powder bed to cause bonding of the particles. The procedure includes multiple steps for spreading a layer of particles on the powder bed and then sintering selective regions of the bed by raster scanning with laser, electron beam or binder jet. This process leads to the fabrication of a component surrounded by loose powder, which is subsequently removed and recycled. Although commercial processes were introduced >30 years ago, it is only in the last decade or so that the growth in the application of AM has really started to take off. However, while the rate of this growth and the level of innovation point to a positive future, many challenges still remain. The ease with which the powder is spread in order to provide a uniform layer (known as 'spreadability') strongly influences the quality of the finished part. Hence, the monitoring and control of the powder spread layer quality is an essential step, and yet is a challenging task, in powder ALM. In general, the quality of the spread layer will depend on:

(i) powder characteristics (i.e. particle size, particle size distribution, particle shape, powder angle of repose, particle mechanical properties and particle aspect ratio): For instance, higher packing densities, smoother surfaces and improved part accuracy can be achieved by widening the size distribution to include a finer fraction, however spreading such distributions can be problematic [1]. On the other hand, Parteli and Pöschel [2] reported that smaller surface roughness was attained after spreading powders with narrow particle size distributions. This is because the fine particle tended to make agglomerates during spreading which cause lower powder bed packing fraction. Ma et al., [3] investigated the effect of adding different volume fractions of fine metal powder (in the range from 20 μm to 40 μm) to a metal powder with a particle size between 45 μm and 150 μm on the powder's bed surface roughness. Adding 1.5% fine particle leads to a decrease (approximately 18%) of the surface roughness. However, adding fine particles larger than 1.5% cause an increase in void content in the powder bed. This is due to the increased cohesive forces between particles in powders with a higher fine fraction.

Meier et al., [4] reported that the powder bed surface roughness increases with increasing powder bulk cohesion. This is attributed to two phenomena, firstly, to the increasing occurrence of particle agglomeration during powder bed spreading, and secondly, to the particles that are ripped out of the powder layer as a results of particle-to-blade adhesion. He et al., [5] investigated the effect of bulk cohesion (particle Bond numbers from Bo = 0 to Bo = 400) on the powder bed surface roughness by using DEM simulation. Surface roughness was low in the Bond number range of 0 to 50, then rose with Bond number.

Haeri et al., [6] used DEM simulation to explore the impact of particle aspect ratio (between 1 and 2.5) on powder bed surface roughness. Higher surface roughness was attained by increasing aspect ratio from 1 to 2.5. Shaheen et al., [7] investigated the influence of altering powder mechanical properties, specifically inter-particle friction (cohesion), sliding and rolling frictions, on powder bed quality using DEM simulation. Changing the particle sliding friction coefficient had a minor impact on layer uniformity, whereas the coefficient of rolling friction had a bigger impact on powder bed uniformity. With a higher coefficient of rolling friction, the powder bed is less homogeneous and more porous. Surprisingly, when both rolling and sliding frictions increased, powder bed quality improved. The authors did not provide an explanation for this behaviour.

(ii) spreader type (flat, rounded blade, elliptical shape blade and roller): Haeri et al., [6] reported that the application of blade shape spreaders causes larger surface roughness compared to the application of roller spreader. In another study Haeri [8] compared surface roughness of powder beds attained by using roller and elliptical shape blade spreaders. The surface roughness of powder bed produced by an elliptically shaped spreader is lower than the roller spreader.

(iii) spreading conditions (i.e. recoater's velocity, gap size, direction of movement and vibration): Blade speed has large impact on powder bed surface roughness, particularly better uniformity is attained when the blade spreader speed is lower than 80 mm/s [9]. Chen et al., [10] reported that powder bed surface roughness were increased monotonically with the increase of a roller recoater spreading speed. Parteli and Pöschel [2] reported that larger roller speed resulted in higher surface roughness. Haeri et al., [6] used DEM to investigate the impact of both blade and roller translational velocity on powder bed surface roughness. They reported that larger translational velocity leads to a higher surface roughness.

Haeri et al., [6] investigated the effects of different gap thickness (distance between the roller spreader tip and powder build plate) on powder bed surface roughness. Higher gap thickness resulted in lower surface roughness. Zang et al., [11] reported that spreading at the gap size at the same range as the tested powder's D_{50} leads to a very low powder bed density. The authors proposed a gap size three times greater than the powder's D_{90} in order to achieve a homogenous powder bed. It should be noted, however, that in the AM industry, the gap size is normally chosen within the same magnitude as the powder's D_{90}.

Beitz et al., [12] investigated the effect of direction of powder deposition on powder bed surface roughness. The surface roughness of the powder bed was not affected from the direction of powder deposition.

(iv) environmental conditions (i.e. high relative humidity and temperature): Both high powder bed build plate temperature and powder temperature are important factors when spreading cohesive powders over the build plate. The effect of temperature should be accounted for by testing at the temperature to be used in the build machine, because many powders show changed behaviour with high temperature [13]. This is mainly done to improve their flow behaviours. For instance, in AM industry, both thermoset powder and build plate temperature are increased in manufacturing for process reasons, which has also a beneficial effect in improving powder flowability.. The spreading machine is kept in a lab with temperature and humidity controls (temperature of 20 °C and Rh%: 40%). As a result, the temperature and humidity between each test were maintained at the same level.

The impact of the environmental factors on powder rheological properties and the powder spreading process has not been thoroughly

explored by researchers. While it has been established that the temperature of the building chamber, the fabrication plate, and humidity all play a role in the thermal process of sintering or melting and solidification of the powder, few studies have investigated how these factors affect the powder spreading process and the relationship between them and the other process parameters [14].Further research into the effect of chamber temperature and relative humidity on powder bed surface roughness is needed. Infact, the authors are taking into account these considerations and plan to include a heating element on both the build plate and the recoater for a future work.

There are considerable reported research works in the literature focusing on quantification of spread powder layer quality and its relation with the above-mentioned parameters (i – iv). However, very few studies developed methods to determine powder bed properties (powder bed surface roughness) by application of image analysis techniques. The percentage of the built plate covered with the powder was assessed by the image taken from the overhead camera by Snow et al. [15]. Sun et al., [16] used image analysis and the shade and bright pixel evaluation technique for AM powder bed characterization. They found that powder with spherical particles makes a more uniform spread layer compared to the powders with elongated particle shapes or recycled powders with small imperfection on the particles' surface. Nan and Ghadiri [17] used image analyses techniques to analyse the size and frequency of the empty patches over the powder bed using ImageJ and MATLAB software. Large empty patches are formed when the gap height is small. Bartlett et al., [18] successfully developed a method to analyse 3D image of the powder bed to identify and quantify the severity of powder bed defects. Grasso et al., [19] proposed a statistical method based on Principal Component Analysis (PCA) to identify defects over the powder bed, by using powder bed image. The main objective of this paper is to report the development of an integrated measurement and monitoring system for the spreading of AM powders to quantify the quality and consistency of the surface of the spread layer in additive manufacturing using a shadowgraphy technique.

1.1. Spreader test rig development

The test rig comprises essentially, four elements

1. The basic structure and machinery to produce the required motions
2. Means for dispensing the powder in controllable quantity and position
3. Means for spreading the powder in a controllable way
4. Means for measuring the quality of the spread layer.

These will be addressed in turn below.

1.1.1. Basic machine elements

A basic requirement of the tester development was to focus on the spreading behaviour of the powders being tested, removing any artefacts of behaviour caused by vagaries in the operation of the spreading machinery. Therefore a decision was made at the outset that the machinery of the test rig must be built with the highest achievable level of precision, accuracy and repeatability. The basic specification identified was as follows:-

1. On the horizontal motion
   a. Freedom from any unintended vertical movement (slack, vibration or other unintended vertical displacement) to a micron level
   b. Controllable speed and travel up to approximately 100 mm/s
   c. Repeatable movement from cycle to cycle
2. On the vertical adjustment
   a. Highly accurate setting and visual indication of the spreading clearance (layer thickness) to within a few microns
   b. Ability to maintain this accurately through many cycles
   c. Ability to adjust and reset the clearance repeatably within a few microns
3. On the spreading surface
   a. A flat surface within a few microns
   b. Ability to change out the surface to explore the effects of surface texture
4. On the relation between elements
   a. The spreading gap to be accurately maintained at the set value across the full width and throughout the length of the travel
5. A structure of sufficient weight and rigidity to damp any vibration from both internal and external sources
6. The above to be achieved within a reasonable cost using as far as possible mass produced components so that the design could be replicated affordably for widespread use.

To satisfy these requirements, it was clear that the device would have to be built to machine tool standards. Consideration was given to available machine tool concepts that are proven to achieve the production of accurately flat, repeatable surfaces and the obvious choice was the surface grinder, which is a widely available tool.

The search for a machine of sufficient accuracy and size at reasonable cost identified a WARCO surface grinder model 2013 YZ. This is a readily available stock item built to suitable standards available at modest price, and could readily be fitted by the supplier with a high accuracy measuring system for vertical displacement known as a Digital Read-Out or DRO, accurate to 5 μm, which is the greatest resolution normally achievable in machine shop or tool-room applications. This was procured and repurposed to form the basic mechanical motions of the spreadability test rig at The Wolfson Centre.

Modifications required to the basic machine were quite limited, involved only removing the grinding head and adding a controlled-speed horizontal drive. The WARCO machine lent itself well to the necessary drive control as it was supplied without a motorised horizontal drive, instead having a capstan intended for manual operation. The capstan was easily removed and a 180 W three phase geared motor added in its place, driven from an inverter variable speed drive unit initiated by manual push button and controlled by limit switches.

This system satisfied all the requirements identified above including the necessary structure and movements, with an outstanding level of mechanical precision well beyond that of previous research test rigs used for powder spreading, for a small fraction of the cost of building a bespoke set-up. In point of fact, the cost of this mass-produced precision machine was substantially less than would have been incurred by purpose-building even an inferior system using the components often employed for such test rigs. As such, this proved to be a very satisfactory solution.

The photograph in Fig. 1 shows the spreadability testing rig together with its full range of functionalities. In Fig. 2 the close-up of mechanical details of recoater blade control elements are shown in detail. In Fig. 3 the details of drive arrangement for horizontal (spreading) motion is depicted.

Note that the front-to-back position adjustment was used only to facilitate pickup of powder using the electrostatic charge analyzer, and left set for spreading.

A cast iron surface plate 150 mm square, ground to accurately equal height across its width and length, was added on top of the horizontal motion table, with the intention of accommodating a heating system in due course to simulate the elevated temperature used in most industrial spreading machines, although this was not added during this project.

1.2. Powder deposition system

Different types of feeding systems are used in the additive manufacturing industry. Some AM machines used a hopper feeding system, while others used a pool feeding system or other feeding system [20]. Each form of powder feeding mechanism has its own set of benefits

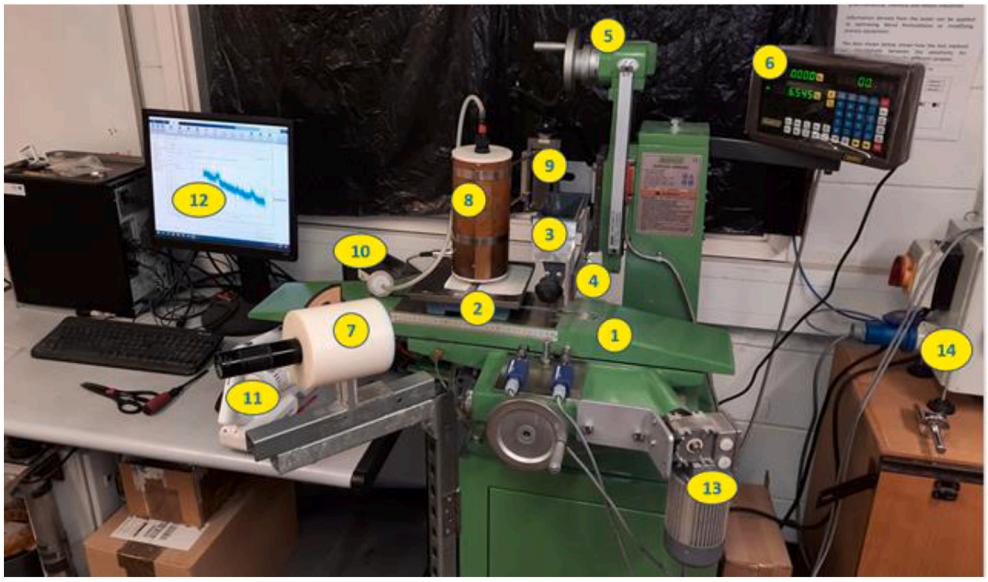

Fig. 1. AM powder spreadability tester based at The Wolfson Centre.
1. Commercial machine frame for x-y-z motion
2. Spread table on moving carriage
3. Powder dispenser
4. Spreader blade
5. Blade-table clearance adjustment
6. Blade-table clearance digital readout
7. Collimated light source
8. Electrostatic sensor (not used in in this paper)
9. Height adjuster for electrostatic sensor (not used in in this paper)
10. Powder filter (not used in in this paper)
11. Vacuum source (not used in in this paper)
12. Computer for data logging (not used in in this paper)
13. Motor drive for carriage
14. Controller for carriage drive

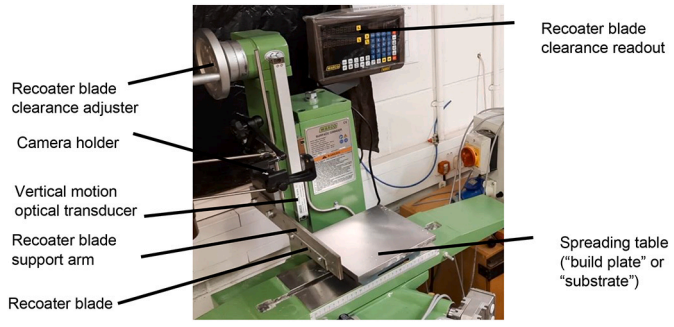

Fig. 2. Close-up of mechanical details of recoater blade control elements.

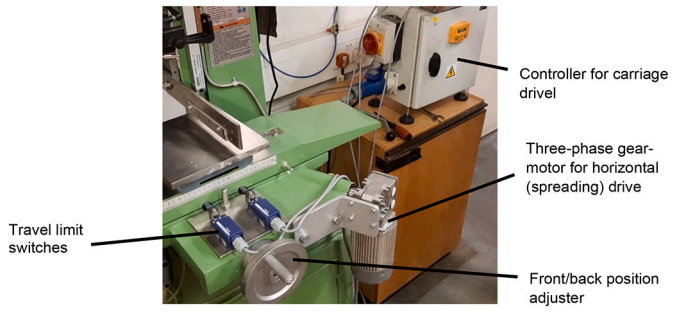

Fig. 3. Details of drive arrangement for horizontal (spreading) motion.

and drawbacks, and can be utilised depending on the application, feeding direction, and powder nature. Different powder feeding systems for AM technologies are classified and reported elsewhere [21]. The different feeding systems in the AM industry raise the question of how the feeding system affects the powder bed quality, which deserve further investigation. This new technique for assessing spread quality gives the opportunity to study these.

A reliable and repeatable technique was required for powder deposition. This would need to be able to deposit a known, controlled volume of powder evenly across the width of the substrate, in front of the recoated blade. Two routes have been explored:

1. Powder hand fed into a chamber of a fixed size, which is then subsequently released onto the powder build plate (or substrate). The dimensions for chamber/trough are determined by assuming 10–20% excess powder and the known gap size.
2. To obtain a more controlled and repeatable quantity and position of deposition, The Wolfson Centre has developed a deposition system (Fig. 4a to d) consisting of a hopper that holds a quantity of powder, above a cylindrical shaft 16 mm diameter with a slot 5 mm wide and 5 mm deep in one side, and from which the powder is then deposited by making one or more turns of the shaft manually using a knob. This technique worked very well for all except two powders, (thermoset and PP2) due to the cohesiveness of these powders, however these limitations could be overcome by further refinement. For these two powders the first method of powder deposition was used. Initially the hopper side plates were manufactured from PVC, but later replaced by steel to reduce adherence of particles due to electrostatic charge. The rotor and stator are manufactured from acetal and PVC respectively, this combination has not shown any problems and gives sufficient mechanical compliance to avoid jamming of the rotor by particles, in spite of the close diametral clearance of approximately 25 μm.

1.3. Powder spreading ("recoater") blades

Two different recoater blade geometries were used in this study. The sketches of the two recoaters are depicted in Fig. 5. The recoater with higher cross sectional area and flat "nose", Fig. 5a, is referred to in this report as recoater configuration 1, or NB. The tapered recoater with the smaller cross sectional area and sharp edge, Fig. 5b, is referred to as recoater configuration 2, or IB. Based on the suggestion from Nan et al. [22] for a suitable gap size two gap sizes were selected; namely 2 times higher than powders D_{90} and 5 higher than the powders D_{90}.

1.4. Measurement of powder layer quality (surface roughness) by shadowgraphy

Shadowgraphy technique based on illuminating the surface with low-angle collimated light and analysing the image was employed to quantify powder bed surface roughness. The light source (see number 7 in Fig. 1) was manufactured from low cost components. This comprised an engineers' quality battery electric LED torch with the head and lens removed to expose the LED source, which was about 1.5 mm across,

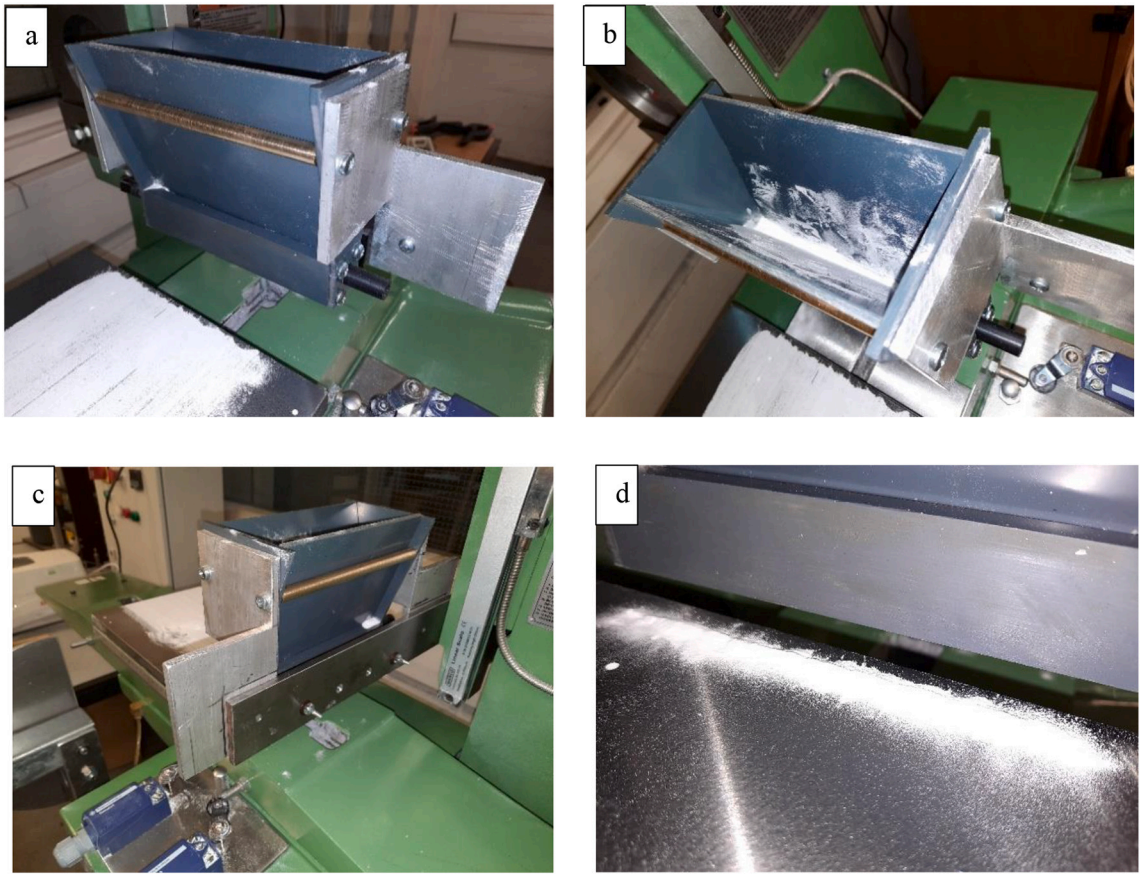

Fig. 4. Powder deposition system. a)the side; b) top view; c) attachment of the powder deposition unit on the recoater blade support bar and d) an example of the controlled quantity of powder deposited in a single turn of the rotor.

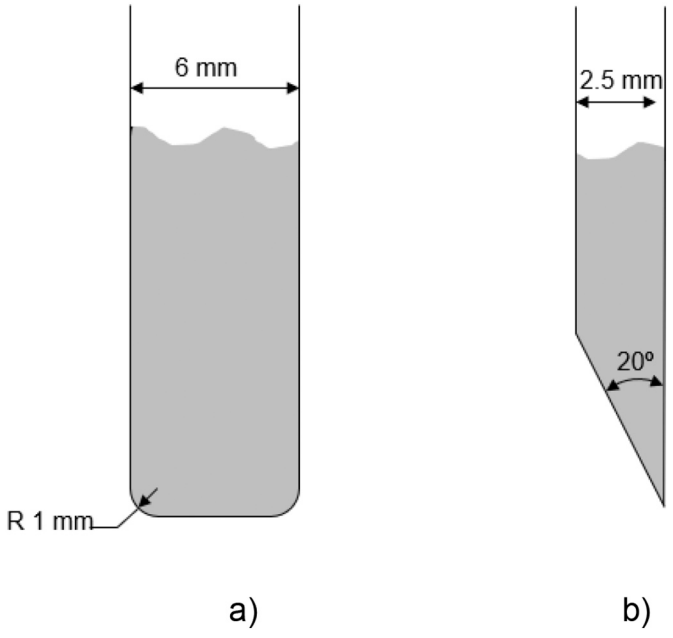

Fig. 5. Two tested recoater shapes. a) recoater configuration 1 or NB; B) Recoater configuration 2, tapered blade, or IB.

which was positioned at the focal point of an 80 mm diameter glass bi-convex lens with a focal length of approx. 100 mm, held together in a custom-made housing machined from polyacetal. Collimation of the light (i.e. parallelism of the rays in the beam) was achieved within about 50 mm over a 3 m length of beam, by minor adjustment of the position of the LED light source. This achievable limit of collimation was a function of the spherical lens design, but this was found to be adequate to give a very even illumination level and angle across the full 150 mm width of the spread. The light source assembly was mounted on a protractor mounting mechanism of a design commonly used on machine saws, giving a rigid, repeatable mounting with an accurate, calibrated angle adjustment. The angle of the light beam to the surface was experimented with and it was found that an angle of 6 degrees gave a good result. The spreading direction and the light direction form a 90-degree angle. To record the image, a cell phone with a high resolution camera was mounted on a bracket (see Fig. 2) affixed above the rest position of the spreading table. The accurate setting of this bracket was found to be important; ensuring the rows of pixels in the image were accurately parallel to the spreading direction helped to improve the resolution of the data analysis.

1.5. Establishing metrics to measure surface roughness

The first objective was to develop metrics to define the quality of the powder layer. To do this, the first step is to take an image of the powder bed using a high definition camera. A collimated light source is projected across the surface of the powder bed, creating a shadowing effect that increases the visual impact of surface topographical differences (see Fig. 6). Images depicting these differences in light intensity ('grey scale') are then digitised using either ImageJ or Matlab software. The intensity of the grey scale of each pixel is then analysed in Excel.

The next step is averaging the grey-scale/brightness intensity of the pixels in the image by taking the average of each column in the direction

Fig. 6. Example of powder bed surface image under 6 degree incident collimated light.

of travel and then the average of 5 rows perpendicular to the direction of travel (see Fig. 7).

The fourth step is to compensate for the variation in brightness of illumination across the overall field of the image. To do this a normalised grey scale value for each pixel is calculated by subtracting the average grey level across 100 pixels, as shown in Fig. 8.

The results of the normalised grey scale for the powder bed image depicted in Fig. 8 is presented in Fig. 9 The depth and width of shadow or peak of brightness links to depth or height of the feature of the powder bed's image.

The two primary metrics which were developed to characterise the powder bed surface quality were:

1. Amplitude of variation in grey scale (Fig. 10) which is defined as the difference between grey scale at each data point and the average grey scale over 100 points ("normalised" in this way to compensate for slight variation in light intensity across the width of the spread pattern). The "mean absolute deviation from the local mean value" is defined as the Ga. This metric is an indication of the 'bumpiness' of the powder bed.

2. Wavelength of roughness (Fig. 11) which is calculated as the average number of pixels between positive peaks, averaged over 100 pixels. Because each pixel has a known dimension, this metric is directly equal to the wavelength of the surface roughness, SA.

Note how the amplitude of the grey scale variation, Fig. 10, captures clearly the presence of a severe trough in the surface, and the visible change in "bumpiness" of the surface as it varied from left to right. The depth of the shadows indicate the depth of the deviation of the surface from a flat plane, and the width of them is the width of these deviations. These reveal variation in the local layer thickness, causing variation in energy input per unit volume of powder in melting or sintering. However, the role of wavelength of the surface texture (Fig. 11) was also considered relevant for the reason that in the case of laser or electron beam melting, the melting process following spreading has a finite size of melt pool; clearly, variation in surface texture on a smaller scale than this melt pool size would have little effect on component quality and vice versa.

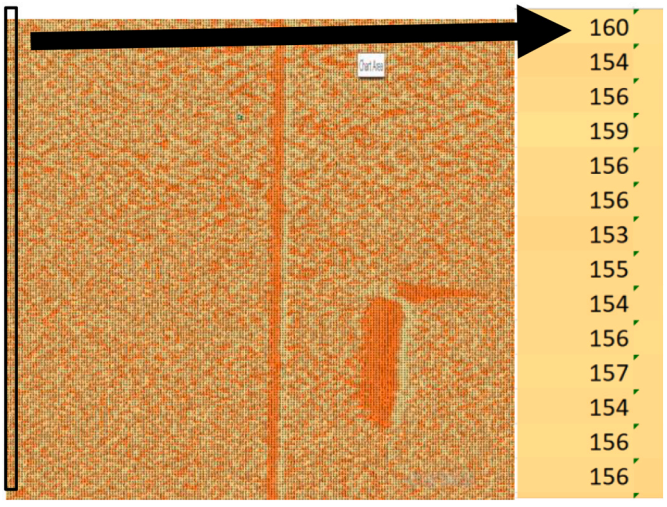

Fig. 7. Averaging the grey-scale/brightness intensity.

At present a human operator is required to transfer the image from the camera to the image capture software, and from there to Excel. However, the full automation of these operations would be a relatively simple software development so no operator intervention would be required in the making of a measurement. This would make the system robust against operator effects and very easy to use. It is necessary for the operator to clean the powder off the spread table after making a measurement. In the results section, the impact of various spreading variables (spreader shape and spreader gap size with the build plate) and powder types on these metrics was thoroughly investigated.

2. Materials

6 different polymer powders were supplied by the Ricoh Company and used in this research work

- Ricoh polypropylene (PP) - spherical particle shape produced by melt emulsification
- PP2 – a polypropylene powder produced with cryogenic milling (cornflake particle shape).
- TIGITAL® SERIES 371 PREMIUM PERFORMANCE (Tiger Coatings), a thermoset powder produced by milling. Referred to Thermoset in the text.
- Polybutylene terephthalate (PBT) powder characterised by cylindrical shape powders, produced with a patented Ricoh process named EMIC (Extended Fibre Micro Cut) which consists in chopping polymer fibres with a very controlled particle size and shape. Referred to PBT in the text.

2 different metal powders were provided by the Carpenter Additive. These powders have more spherical particles compared to the polymer powders provided by Ricoh.

- LPW-TI64GD23-AAFD-UK3324 (Referred to TI in the text)
- LPW-ALSI10MG-28-GR1–12412 (Referred to AL in the text)

2.1. Powder characterization results

1. Flow Function

The flow properties of the powders were measured by the Brookfield Powder Flow Tester (PFT, Brookfield Engineering Laboratories, Inc., Middleboro, MA, US) [23]. It's a ring shear tester with a similar measurement principle to the Schulze tester. The tester's operation and extensive descriptions have been published elsewhere [24]. The number of consolidation points (i.e. the number of yield loci) and over-consolidation points (i.e. the number of points in each yield locus) were set to 4 and 5 respectively. Jenike explains how to use the shear tester to determine the flow parameters of powders [25]. The curve that fits through the yield loci points represents powder flowability. The Jenike flowability classification using the Flow Function value, $ff_c = \sigma_1/f_c$, the major principal stress as a function of the unconfined yield strength, is a commonly used method for reporting powder flowability. The classes generally considered are the free flowing ($ff_c \geq 10$ or $1/ff_c < 0.1$), easy flowing ($4 < ff_c \leq 10$ or $0.1 < 1/ff_c < 0.25$), cohesive ($2 < ff_c \leq 4$ or $0.25 < 1/ff_c < 0.5$), very cohesive ($1 < ff_c \leq 2$ or $0.5 < 1/ff_c < 1$) and non-flowing ($ff_c \leq 1$ or $1/ff_c > 1$).

The unconfined yield strength of all tested powders as a function of the major principal stress is shown in Fig. 12. Eq. 1 calculates the unconfined failure strength as a function of both the friction angle, φ_i, and the powder cohesion, c. As a result, the results of bulk cohesion and friction angle were not reported in this paper.

$$f_c = 2c\frac{cos\varphi_i}{1 - sin\varphi_i} \quad (1)$$

Comparing the results from the plastic powders, shows that all

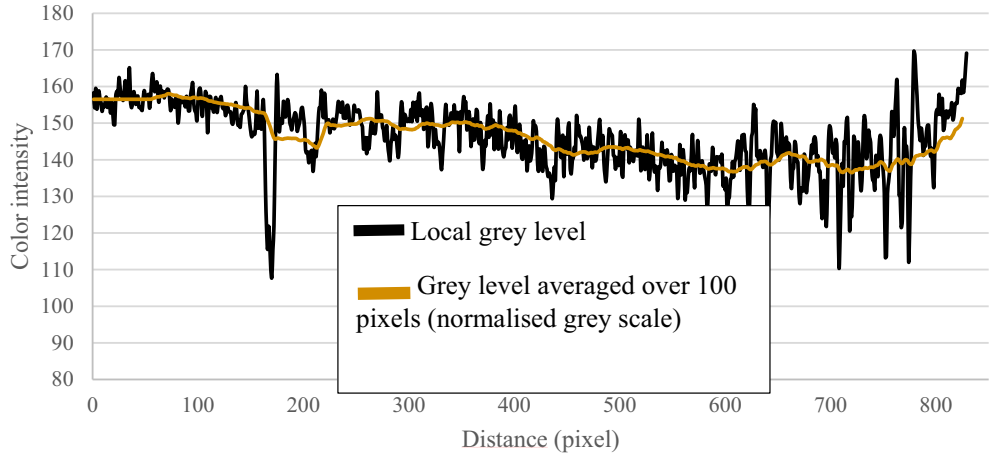

Fig. 8. The difference between the local grey level and the 100-pixel average is recorded as the normalised grey scale.

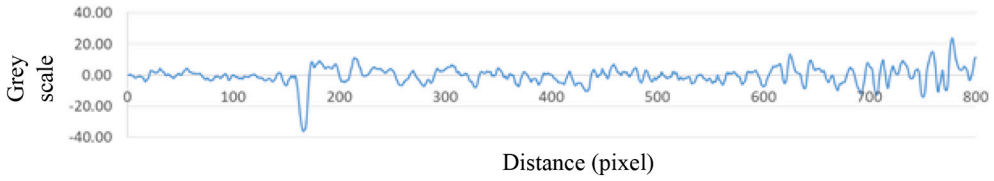

Fig. 9. Normalised Grey Scale Values (compensated for small variation in light intensity across the width).

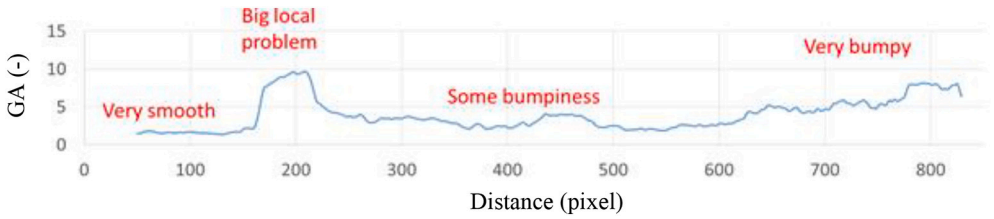

Fig. 10. Local amplitude of Grey Scale Values.

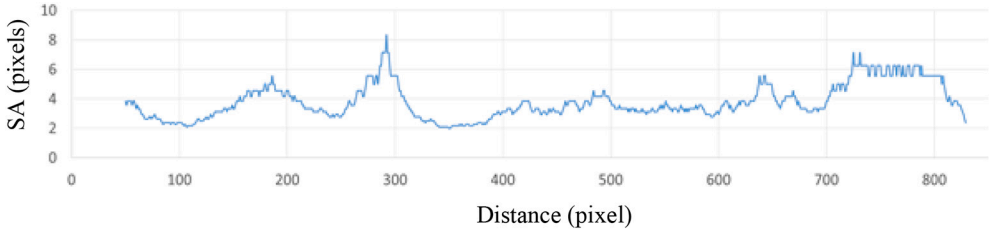

Fig. 11. 'Wavelength of Roughness' - Distance between Peaks.

powders except Ricoh PP were classified as an easy-flowing powder. Ricoh PP was the most free flowing powder compared to the other plastic powders. The flow functions of all metal powders are classified as a free flowing powder with a slight tendency towards easy flowing region at low consolidation stress.

2. Particle size distributions

Particle size distribution measured with a laser diffraction particle size analyzer (Malvern, Mastersizer Sirocco 2000) with Sirocco dry powder feeder and using dry air as the dispersion medium. The data derived from the Mastersizer is presented in Table 1. D_{10} (μm), D_{50} (μm), and D_{90} (μm) based on spheres of equivalent volume to the particles. D_{50} is the volume median of the particle size distribution, which is used as the mass median under the premise that all particles have the same density. D_{10} is the particle size below which 10% of the sample mass falls and D_{90} is the size below which 90% of the sample mass falls, based on the same assumptions as for D_{50}.

3. Particle shape

The SEM images of the tested powders are depicted in Fig. 13. Thermoset and PP2 have irregular shape particles, PBT has the cylindrical shape particles, Ricoh-PP has spherical and oval shape particles and the two metal powders (AL and TI) have spherical shape particles.

2.2. Shadowgraph technique: metrics developed to define surface roughness

The same segment size from each of the powder bed image was

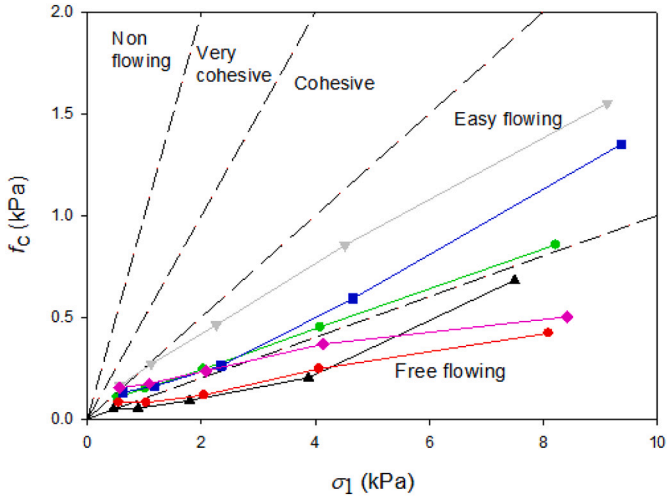

Fig. 12. Flow function of the tested powders PP2 (■ —) Ricoh-PP (▲ —) Thermoset (▼ —) PBT (● —) TI (♦ —) and AL (● —).

Table 1
Particle size distribution of the tested powders.

Material	D_{10} (μm)	D_{50} (μm)	D_{90} (μm)
Ricoh PP	28	49	85
PP2	42	84	139
Thermoset	15	44	80
PBT	52	70	95
AL	27	50	83
TI	28	54	85

cropped using ImageJ. The surface roughness metrics can be calculated across the entire surface, however because many defects and deficiencies in layer quality appear to be localised, it appears to be more useful to calculate both metrics on a smaller base length across the surface, so that the variation of the roughness across the spread surface can be plotted and problem areas identified and quantified. Fig. 14 demonstrates an example of the powder bed surfaces of one titanium metal powder (LPW-TI64GD23-AAFD-UK3324) (TI) and PP2 plastic powder both spread with the IB recoater at a bed depth of $2*D_{90}$. Figs. 1 and 2 in appendix summarized all images of the powder beds attained at the bed depth of $2*D_{90}$ and $5*D_{90}$, respectively.

It is clear from the images that the PP2 powder suffers a deeper surface roughness, as indicated by the greater range of lightness and darkness, but also this roughness is at a larger scale as indicated by the greater distance between the bright and dark areas. Both of these effects are captured faithfully in the "Amplitude of grey scale roughness" and the "Wavelength of roughness" reported in Table 2. This demonstrating the ability of this measurement technique and metrics to capture the difference in surface texture.

The SA values of all tested powders spread with either IB or NB recoaters are depicted in Fig. 15a for the gap size $2*D_{90}$ and in Fig. 15b for the gap size of $5*D_{90}$. The GA values of all tested powders spread with either IB or NB recoaters are depicted in Fig. 15c for the recoater gap size $2*D_{90}$ and in Fig. 15d for the gap size of $5*D_{90}$. Thermoset and PP2 are the most cohesive powders compared to the other tested plastic powders. As expected, spreading powders with high value of bulk cohesion leads to a powder bed with high surface roughness. This behaviour of powder leads to higher surface roughness of these two powders compared to the other tested powders. Powder beds with higher surface roughness have higher SA and GA values than powder beds with better flowability. For example, the GA and SA values of Thermoset and Reposl powder beds are the highest when compared to the SA and GA values of the most free flowing powder (Ricoh PP). This result is consistent with the findings of Sun et al., who observed that improved powder flowability, i.e. lower $1/ff_c$, resulted in a more homogeneous layer in AM. [16]. Also Ma et al., reported that large number of voids are formed over the build plate when spreading powders with low flowability, i.e. high $1/ff_c$ [3].

Inspection of surface roughness metrics results depicted in Fig. 15 revealed that, in general, spreading plastic powders with NB (broad nosed) recoater resulted in somewhat slightly higher surface roughness compared to the condition where the powders were spread with IB (sharp edged) recoater at gap size $2*D_{90}$. This demonstrates that using the NB recoater results in a bumpy powder bed as compared to using the IB recoater. Surprisingly, spreading cohesive plastic powders at the gap size of 5 times higher than D_{90} leads to a higher surface roughness compared to the condition where the powders were spread at the gap size of two times the powder's D_{90}. This might be due to the fact that larger particles can pass through the gap size between the recoater and powder bed at the gap size 5 times higher than the D_{90}. When the large, irregular and rigid particles (see Fig. 13, PP2 and thermoset) pass through the recoter gap, they may cause the formation of imperfection at the powder bed, i.e. valleys and heights. On the other hand, the large, irregular and rigid particles cannot pass through the recoater gap size of at $2*D_{90}$. Hence, these particles are 'snow ploughed' and cannot deposited and/or cause imperfection over the powder bed.

The inspection of the surface roughness of the powder bed formed from spreading the metal powders showed lower SA and GA than the surface roughness of the surface bed of the plastic powders. This might be due to the lower $1/ff_c$ of these powders compared to plastic powders (see Fig. 12). Other contributory factors may be that the metal particles have much more spherical shape than the plastic particles (see Fig. 13), allowing them to move more easily, and also a higher weight, giving more force to hold them down. Spreading powders with larger amount of spherical particles leads to a higher powder packing density and lower surface roughness.

2.3. *Calibration of the surface measurement technique to reveal actual surface feature height or depth*

At an early stage it was apparent that the extent of the grey scale variation appeared to be linked to the height and depth of the surface irregularities, but it would be important to establish what this relationship was in order to obtain meaningful measurements.

It was desired to calibrate the shadowgraphy technique to deliver absolute metrology values of powder bed surfaces, in terms that would be understood by a mechanical engineer. The most commonly used metric for surface roughness in engineering is "Roughness Average" or "Ra" which indicates the average deviation of the high and low peaks and troughs from a median surface, determined over a defined length. This is what is most usually measured using engineering surface measuring equipment such as the ubiquitous "Talysurf" from Taylor Hobson, and equivalent instruments, but these instruments cannot be used on a powder surface as they rely on a stylus moving over a solid surface with a contact force. The next most popular metric is wavelength of the surface roughness, again using the same measuring technique, calculated as the average distance between peaks along the same defined length of the surface; the name for this metric varies but in this report the term "SA" will be used. Both values are normally expressed in microns or decimals of a millimetre, except in the USA where "mils" (milli-inches) are normally used. NOTE: Care must be taken when making comparisons, not to confuse the US "mils" with the slang term "mil" for millimetre common in UK engineering practice, because they are different by a factor of 40. The perceived value of these measurements to consideration of the adequacy of the surface for sintering or melting is discussed above in section above.

It would not be possible to use a contact measuring device on a loose

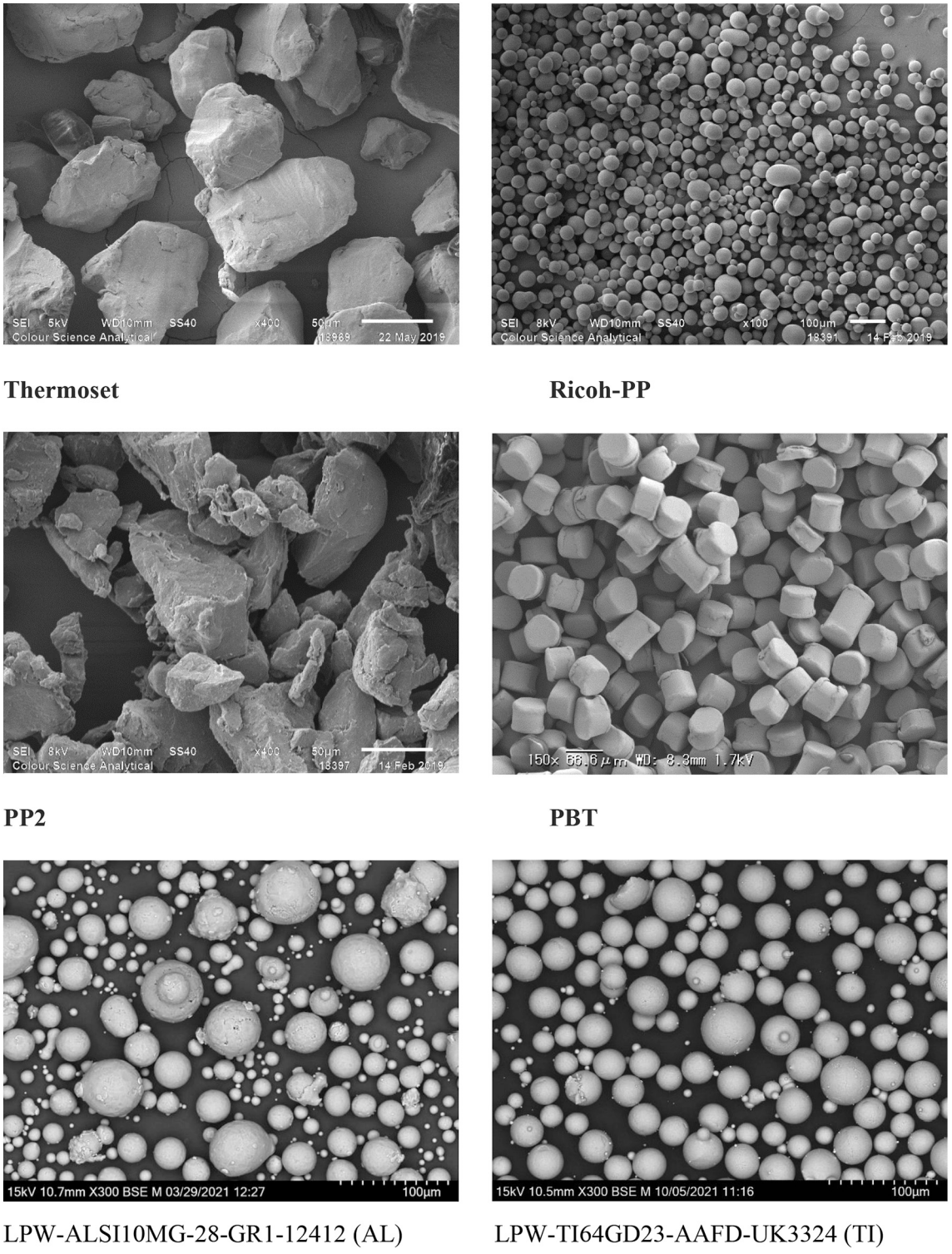

Fig. 13. Microscopic image of the tested powders.

powder surface. In principle, laser non-contact surface metrology might potentially be used, so suppliers of such instruments were approached, but they had no experience of their use on a powder surface and did not have confidence that they would deliver reliable measurements from such a surface. Given the high cost of such instruments as well as the lack of confidence in their use in this application, this did not appear to be a promising line of inquiry. Consequently a different approach was taken for calibration, to create surfaces with a known cyclical roughness and wavelength by spreading powders using calibrated recoater blades. For this purpose, saw blades with different numbers of teeth per inch (TPI) were used; namely 10, 14, 18, 24 and 32 TPI (pitches of 2.54, 1.81, 1.31, 1.06 and 0.79 mm respectively). These are readily available at low cost, although made with a high degree of precision.

The use of these saw blades with a sufficiently free-flowing powder would clearly create a surface roughness wavelength equal to the pitch. In terms of the depth of the ridges, the saw blades have an asymmetric tooth shape with an angle of around 45 degrees on the back (shallow) side and a reverse angle (cutting rake angle) of about −5 degrees on the

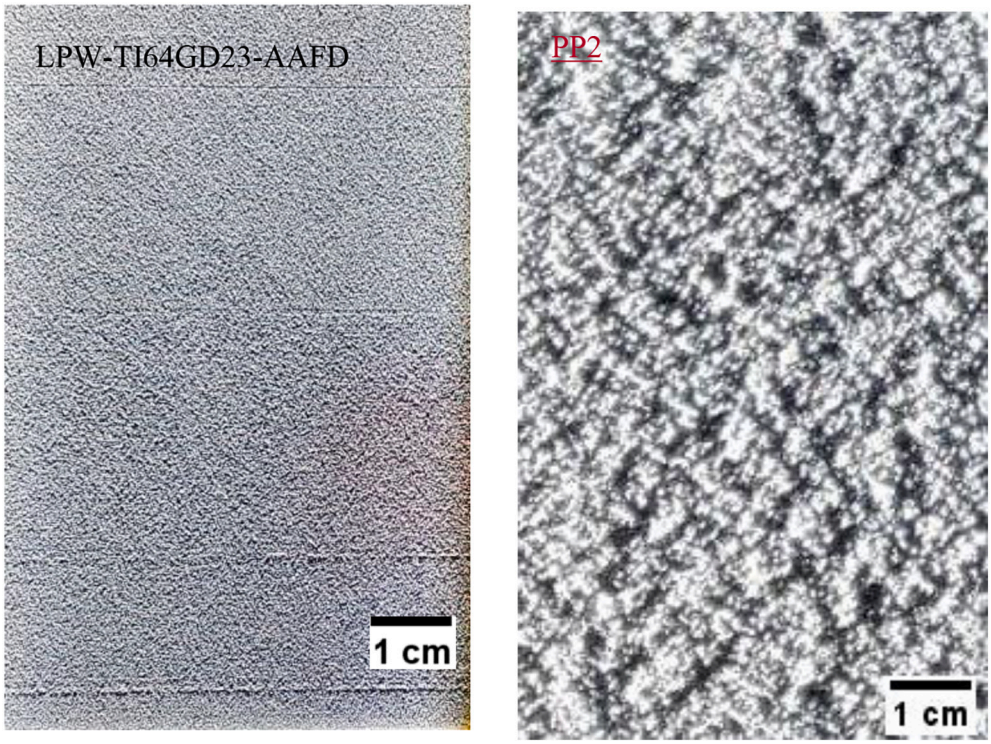

Fig. 14. The powder bed surfaces of one metal powder (TI) and PP2 powder both spread with the IB recoater at 2^*D_{90}.

Table 2
The developed metrics to quantify powder bed surface roughness.

Amplitude of grey scale roughness (–)	Wavelength of roughness (Pixel)	
PP2	11.09	14.19
Titanium powder	4.74	7.79

front side. However, a powder cannot support an angle steeper than its angle of repose, so it was felt to be sufficiently reliable in the first instance to take the view that the powder would assume its natural angle of repose on both sides of the valley formed by the passage of a saw tooth. The depth of the valleys was therefore taken to be defined by the wavelength and the angle of repose as shown in Fig. 16.

The same procedure described above, Surface Roughness Measurement Approach, was followed to obtain the GA and SA values of the surface bed. Knowing the TPI number of each saw blade, the pitch size and the groove depth can be easily calculated. Ricoh PP was used for the calibration, classified as a free flowing powder. An example of Ricoh PP powder bed image using the- saw blade of 10 TPI (2.5 mm pitch) and using normal ambient illumination is depicted in Fig. 17a, and again in Fig. 17b with the low angle collimated light applied, to show the illuminating effect of the lighting system used. Results of the GA and SA values of Ricoh PP powder as the function of groove depth are reported in Fig. 18. The value of "GA" (grey scale average deviation) on Fig. 18a is calculated using the same method as normally used for Ra. The wavelength on graph 18b is in terms of number of pixels.

The strong linear relationship showed that the data derived from the image analysis correlates very well with the surface features created, giving confidence that absolute (i.e. real-world dimension) values of the Ra and wavelength can be extracted from the shadowgraph image using this calibration method.

The scatter in the experimental data at the smaller feature sizes appeared to be caused by the difficulty in creating accurate features of this smaller size in the surface. Even with a very free flowing powder, it does not flow so reliably into a regular texture shape at these smaller dimensions. This was apparent from visual examination of the images, which revealed an increasing incidence of imperfections in the ridged surface with reducing blade pitch. This suggests that the calibration is best undertaken in practice with the larger pitch blades.

The consistency of the calibration across couple of other free flowing powders were also examined. The results showed that the calibration is specific to the powder being processed, due to variations in reflectiveness of the powder surfaces. Therefore a new calibration would need to be undertaken or at least checked, for any new powder being spread. Calibration will be specific to the material due to differences in angle of repose and particle size affecting the light and shadows. Results of the GA and SA values of Aluminium powder as the function of groove depth are reported in Fig. 19.

3. Conclusion

A "spreadability tester" was successfully developed to measure the quality of powder bed surface in the powder ALM process. The developed tester and the techniques were successfully used to quantify powder bed surface roughness. Other powder bed properties, such as relative packing fraction, particle size and shape fluctuation throughout the build plate, and electrostatic charge measurement, were also successfully evaluated using the built tester; however, they were tested using different methodologies than surface roughness. These findings will be the focus of a subsequent publication. The method of shadowgraphy under low angle collimated light has proven to be able to disclose, capture and objectively quantify common defects in powder layer surface quality at a meaningful scale. This technique has the potential to easily be applied in two ways:

- In a build machine to give real time quality control on layers between spreading and fusion/sintering; due to no disturbance of the layer, if acceptable the layer can then be processed or if defects are revealed, it can be recoated again.
- As a "spreadability tester" instrument (the machine set-up developed in this study) for powder characterization in relation to its likelihood to produce defects.

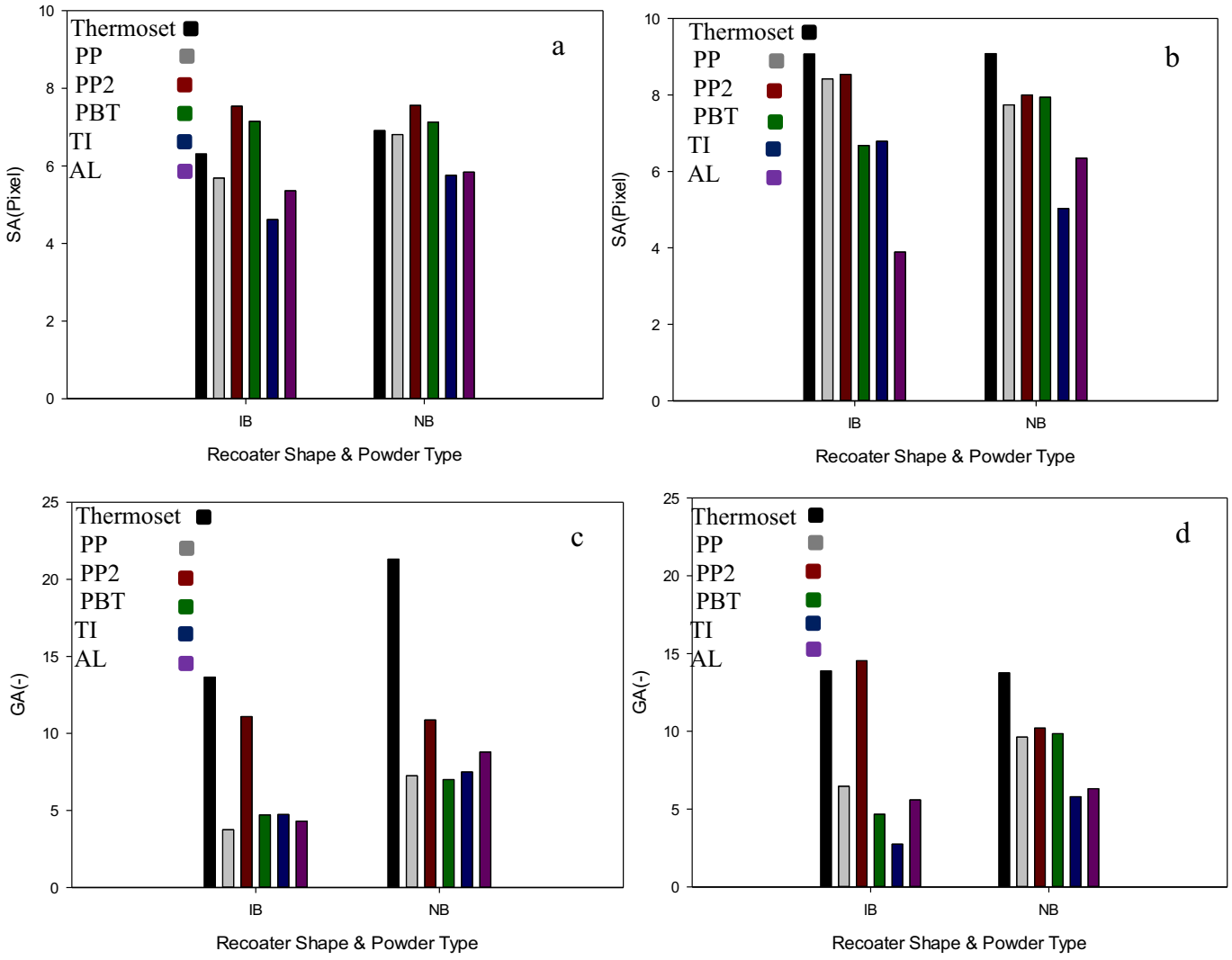

Fig. 15. SA value of the powder beds attained using shadography technique; a) powder bed at gap size $2*D_{90}$ and b) powder bed at gap size $5*D_{90}$. GA value of the powder beds attained using shadography technique; c) powder bed at gap size $2*D_{90}$ and d) powder bed at gap size $5*D_{90}$.

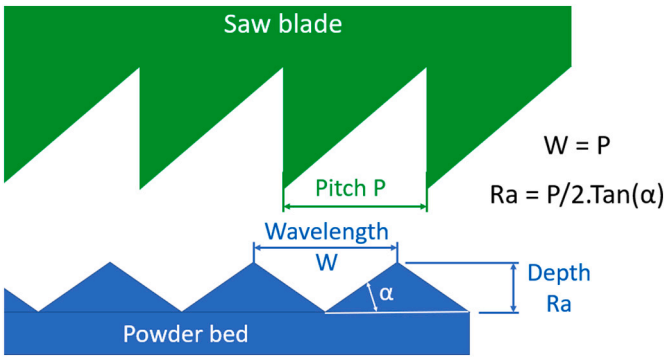

Fig. 16. Calculation of reference calibration bed geometry from known pitch of saw blade and powder angle of repose.

Two metrics have been identified to quantify the powder bed surface roughness; Namely Amplitude of variation in height (GA) and Wavelength of roughness (SA). The amplitude of the height variation captures clearly the presence of a severe trough in the surface, and the visible change in "bumpiness" of the surface. Wavelength of roughness is an indication of the lateral scale of the variation in surface texture.

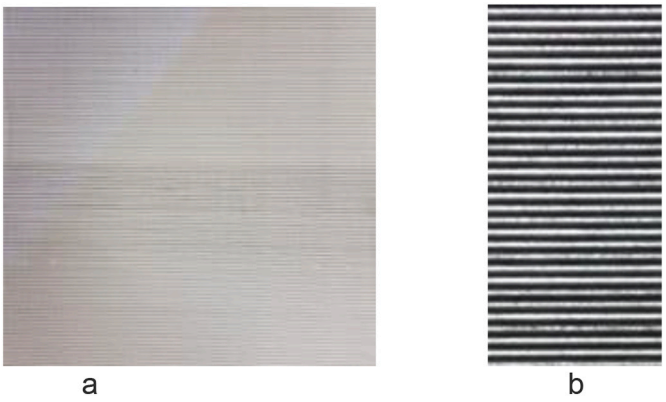

Fig. 17. An example of Ricoh PP powder bed using saw blade of 2.54 mm pitch; photographed using a) normal ambient illumination, and b) with low angle collimated light, scaled and cropped with known dimension. Spreading is done from left to right. Collimated lightning is applied from the bottom up.

Spreading the powder with sawblades with different tooth pitch shows that the technique can be calibrated to absolute dimensional measurements of the depth and width of the defects.

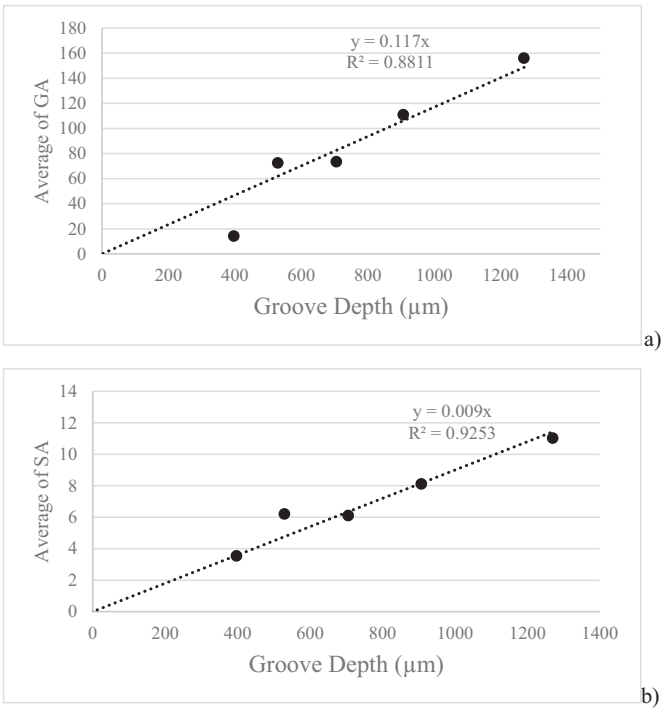

Fig. 18. GA and SA value of powder bed as a results of spreading Ricoh PP powder with sawblade with different teeth number/in..

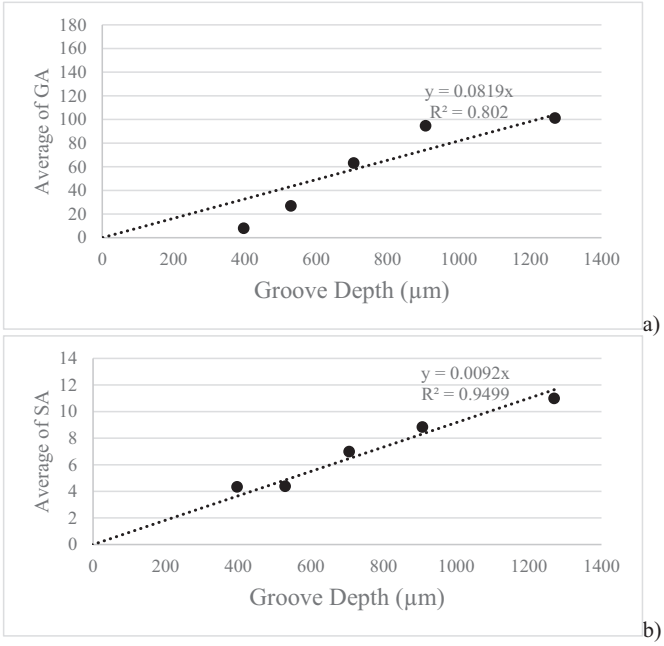

Fig. 19. GA and SA value of powder bed as a results of spreading Aluminium powder with sawblade with different teeth number/in..

In this study 3 types of common defects have been observed:

- o The scale of the random surface texture effects across an area
- o Linear defects along the direction of spreading
- o Excessively low bulk density or packing of the particles

The results showed that the scale of random surface texture correlates strongly with the cohesiveness of the powder as measured using a shear tester, more cohesive powders producing a rougher texture and vice versa. Linear defects (grooving) in the surface are extremely common; it could be due to the imperfections in the recoater blade, but more commonly they are a random effect that probably links to jamming of particles in the heap in front of the blade. Furthermore, the presence of some larger agglomerates in the powder, which is likely in recycled material as it is not normally sieved down to the top size of the original powder, will clearly be highly influential in initiating this form of failure especially if the particles are larger than the recoater clearance. Linear defects have not shown obvious signs of being influenced by the cohesiveness of the powder, although this would benefit from further examination. The depth of the bed appears to influence the depth of the grooving, greater in absolute terms in a deeper bed but not necessarily greater proportionate to bed depth, which may be more important for fusing energy density. There is a much wider effect of powder cohesiveness on spreading, which has been shown up by the tests. For instance, higher $1/ff_c$ of thermoset causes larger number of defects over the build plate. It will be very useful to test finer powder with this techniques to better understand the impact of cohesiveness on the limit of spreadability.

It has been shown that the relationship between the variables involved in the powder, the machine and the process settings, and how these lead to unsatisfactory spreading, is not only complex, but appears to be interlinked. Both the magnitude and direction of the effect of any one variable depends on the values of many other variables. This has a number of important consequences:

- o Studies that attempt to expose the effect of any one variable may produce convincing results in terms of correlation and/or theory, for the case where all other variables are invariant, but are unlikely to be able to be generalised across situations where any other variables at all have different values. Therefore it is imperative that in industrial practice, for both quality control and process planning purposes, powder "spreadability" should be measured using an instrument that can be set up to conduct spreading tests under conditions reflecting those in use of the powder, to obtain meaningful information on how that powder is likely to perform.
- o An analysis of size distribution that can identify a small number of larger particles may give a guide to potential for linear defects (grooving). However, these do not tell the whole story so they may have some function as a quality control measure but only against certain specified problems.

CRediT authorship contribution statement

Hamid Salehi: Conceptualization, Methodology, Validation, Formal analysis, Investigation, Writing – original draft, Visualization, Project administration. **John Cummins:** Conceptualization, Methodology, Validation, Formal analysis, Investigation, Writing – review & editing, Project administration. **Enrico Gallino:** Methodology, Validation, Formal analysis, Investigation, Writing – review & editing, Resources. **Neil Harrison:** Investigation, Writing – review & editing, Resources. **Ali Hassanpour:** Conceptualization, Methodology, Validation, Formal analysis, Investigation, Writing – review & editing. **Mike Bradley:** Conceptualization, Methodology, Validation, Formal analysis, Investigation, Writing – review & editing, Supervision, Funding acquisition, Project administration.

Declaration of Competing Interest

The authors declare that they have no known competing financial interests or personal relationships that could have appeared to influence the work reported in this paper.

Acknowledgements

We Thank The EPSRC Future Manufacturing Hub in Manufacture

using Advanced Powder Processes (MAPP) for providing the grant for this study.

Appendix A. Supplementary data

Supplementary data to this article can be found online at https://doi.org/10.1016/j.powtec.2022.117614.

References

[1] R.D. Goodridge, K.W. Dalgarno, D.J. Wood, Indirect selective laser sintering of an apatite-mullite glass-ceramic for potential use in bone replacement applications, Proc. Inst. Mech. Eng. Part H J. Eng. Med. (2006), https://doi.org/10.1243/095441105X69051.
[2] E.J.R. Parteli, T. Pöschel, Particle-based simulation of powder application in additive manufacturing, Powder Technol. (2016), https://doi.org/10.1016/j.powtec.2015.10.035.
[3] Y. Ma, T.M. Evans, N. Philips, N. Cunningham, Numerical simulation of the effect of fine fraction on the flowability of powders in additive manufacturing, Powder Technol. (2020), https://doi.org/10.1016/j.powtec.2019.10.041.
[4] C. Meier, R. Weissbach, J. Weinberg, W.A. Wall, A.J. Hart, Critical influences of particle size and adhesion on the powder layer uniformity in metal additive manufacturing, J. Mater. Process. Technol. (2019), https://doi.org/10.1016/j.jmatprotec.2018.10.037.
[5] Y. He, A. Hassanpour, A.E. Bayly, Linking particle properties to layer characteristics: discrete element modelling of cohesive fine powder spreading in additive manufacturing, Addit. Manuf 36 (2020) 101685, https://doi.org/10.1016/j.addma.2020.101685.
[6] S. Haeri, Y. Wang, O. Ghita, J. Sun, Discrete element simulation and experimental study of powder spreading process in additive manufacturing, Powder Technol. 306 (2017) 45–54, https://doi.org/10.1016/j.powtec.2016.11.002.
[7] M.Y. Shaheen, A.R. Thornton, S. Luding, T. Weinhart, Discrete particle simulation of the spreading process in additive manufacturing, 8th Int. Conf. Discret. Elem. Methods, 2019, pp. 1–12.
[8] S. Haeri, Optimisation of blade type spreaders for powder bed preparation in Additive Manufacturing using DEM simulations, Powder Technol. 321 (2017) 94–104, https://doi.org/10.1016/j.powtec.2017.08.011.
[9] A. Mussatto, R. Groarke, A. O'Neill, M.A. Obeidi, Y. Delaure, D. Brabazon, Influences of powder morphology and spreading parameters on the powder bed topography uniformity in powder bed fusion metal additive manufacturing, Addit. Manuf. 38 (2021), 101807, https://doi.org/10.1016/j.addma.2020.101807.
[10] H. Chen, Y. Chen, Y. Liu, Q. Wei, Y. Shi, W. Yan, Packing quality of powder layer during counter-rolling-type powder spreading process in additive manufacturing, Int. J. Mach. Tools Manuf. (2020), https://doi.org/10.1016/j.ijmachtools.2020.103553.
[11] J. Zhang, Y. Tan, T. Bao, Y. Xu, X. Xiao, S. Jiang, Discrete element simulation of the effect of roller-spreading parameters on powder-bed density in additive manufacturing, Materials (Basel). (2020), https://doi.org/10.3390/ma13102285.
[12] S. Beitz, R. Uerlich, T. Bokelmann, A. Diener, T. Vietor, A. Kwade, Influence of powder deposition on powder bed and specimen properties, Materials (Basel). 12 (2019) 297, https://doi.org/10.3390/ma12020297.
[13] H. Salehi, R. Berry, R. Farnish, M. Bradley, Temperature and time consolidation effect on the bulk flow properties and arching tendency of a detergent powder, Chem. Eng. Technol. 43 (2020) 150–156, https://doi.org/10.1002/ceat.201900092.
[14] P. Avrampos, G.C. Vosniakos, A review of powder deposition in additive manufacturing by powder bed fusion, J. Manuf. Process. 74 (2022) 332–352, https://doi.org/10.1016/J.JMAPRO.2021.12.021.
[15] Z. Snow, R. Martukanitz, S. Joshi, On the development of powder spreadability metrics and feedstock requirements for powder bed fusion additive manufacturing, Addit. Manuf. (2019), https://doi.org/10.1016/j.addma.2019.04.017.
[16] Y.Y. Sun, S. Gulizia, C.H. Oh, C. Doblin, Y.F. Yang, M. Qian, Manipulation and characterization of a novel titanium powder precursor for additive manufacturing applications, JOM. 67 (2015) 564–572, https://doi.org/10.1007/s11837-015-1301-3.
[17] W. Nan, M. Ghadiri, Numerical simulation of powder flow during spreading in additive manufacturing, Powder Technol. (2019), https://doi.org/10.1016/j.powtec.2018.10.056.
[18] J.L. Bartlett, A. Jarama, J. Jones, X. Li, Prediction of microstructural defects in additive manufacturing from powder bed quality using digital image correlation, Mater. Sci. Eng. A 794 (2020), 140002, https://doi.org/10.1016/J.MSEA.2020.140002.
[19] M. Grasso, V. Laguzza, Q. Semeraro, B.M. Colosimo, In-process monitoring of selective laser melting: spatial detection of defects via image data analysis, J. Manuf. Sci. Eng. Trans. ASME. 139 (2017), https://doi.org/10.1115/1.4034715.
[20] A. Tamura, T. Fujita, A. Takeuchi, Selective powder feeding system in additive manufacturing using laser-induced forward transfer technique, Addit. Manuf. 46 (2021), https://doi.org/10.1016/j.addma.2021.102226.
[21] Y. Patil, A.K. Patel, A. Goutam, S. Chavan, M. Pandya, M. Malaiya, K. P. Karunakaran, Powder Feeding Mechanisms in Additive Manufacturing: A Review, in, 2020, https://doi.org/10.1007/978-981-15-7827-4_69.
[22] W. Nan, M. Pasha, T. Bonakdar, A. Lopez, U. Zafar, S. Nadimi, M. Ghadiri, Jamming during particle spreading in additive manufacturing, Powder Technol. (2018), https://doi.org/10.1016/j.powtec.2018.07.030.
[23] R. Berry, M. Bradley, R. McGregor, Brookfield powder flow tester - results of round robin tests with CRM-116 limestone powder, Proc. Inst. Mech. Eng. Part E J. Process Mech. Eng. 229 (2014) 215–230, https://doi.org/10.1177/0954408914525387.
[24] H. Salehi, D. Barletta, M. Poletto, A comparison between powder flow property testers, Particuology. 32 (2017) 10–20, https://doi.org/10.1016/j.partic.2016.08.003.
[25] A. Jenike, Storage and flow of solids. Bulletin no. 123, USA Eng. Exp. Station. Univ. Utah, 1964.